Investigation of the Thermal and Photochemical Reactions of Ozone with 2,3-Dimethyl-2-butene

Bridgett E. Coleman and Bruce S. Ault*

Department of Chemistry, University of Cincinnati, Cincinnati, Ohio 45221, United States

Received: September 5, 2010; Revised Manuscript Received: October 24, 2010

The matrix isolation technique, combined with infrared spectroscopy and twin jet codeposition, has been used to characterize intermediates formed during the ozonolysis of 2,3-dimethyl-2-butene (DMB). Absorptions of early intermediates in the twin jet experiments grew up to 200% upon annealing to 35 K. A number of these absorptions have been assigned to the elusive Criegee intermediate (CI) and secondary ozonide (SOZ) of DMB, transient species not previously observed for this system. Also observed was the primary ozonide (POZ), in agreement with earlier studies. The wavelength dependence of the photodestruction of these product bands was explored with irradiation from $\lambda \geq 220$ to ≥ 580 nm. Merged jet (flow reactor) experiments generated "late" stable oxidation products of DMB. A recently developed concentric jet method was also utilized to increase yields and monitor the concentration of intermediates and products formed at different times by varying the length of mixing distance ($d = 0$ to -11 cm) before reaching the cold cell for spectroscopic detection. Identification of intermediates formed during the ozonolysis of DMB was further supported by [18]O and scrambled [16,18]O isotopic labeling experiments as well as theoretical density functional calculations at the B3LYP/6-311++G(d,2p) level.

Introduction

The reaction between ozone and volatile organic compounds (VOCs) has sparked an interest in the study of specific chemical systems in the earth's troposphere.[1,2] While ozone does not react appreciably with alkanes in the troposphere, it plays a significant role in the removal of alkenes that arise from both biogenic and anthropogenic sources.[3−6] Early work done by Rudolf Criegee yielded a proposed mechanism for this reaction, shown in Figure 1.[7,8]

Through extensive experimental and theoretical evidence, this mechanism is now widely accepted.[9−12] The mechanism involves the initial formation of a primary ozonide (POZ) by a 1,3 polar addition across the double bond of the alkene, forming a 1,2,3-trioxolane species. This reaction is quite exothermic, leading to further reaction and decomposition of the POZ into a carbonyl compound and the proposed Criegee intermediate (CI), a carbonyl oxide. The CI and the carbonyl compound may then recombine to form a secondary ozonide (SOZ) (1,2,4-trioxolane) or react further to form a range of products.

Experimental and theoretical studies involving the isolation of the SOZ for numerous systems have supported the Criegee mechanism. However, the POZ, CI, and SOZ have only been isolated and characterized for a very small number of alkenes.[13,14] Theoretical calculations have shed additional light on the nature of the reaction as well as reasons for difficulties in observing the CI.[9−12] Theoretical studies have shown that the activation barrier connecting the POZ to the CI is about 19 kcal mol^{-1}. The POZ is formed with nearly 50 kcal mol^{-1} of excess energy, and it can easily continue over the barrier to form the CI and carbonyl compound if not rapidly deactivated. This pair will also be formed with excess energy and must be quickly deactivated and stabilized, or they will react further to form the numerous known products. One pathway to stabilization is ring formation, yielding the SOZ, a 1,2,4-trioxolane.

Matrix isolation[15,16] was developed and has been employed for the isolation and characterization of a wide range of reactive intermediates, including radicals, ions, and molecular complexes. This approach has been used successfully by many laboratories to isolate novel short-lived species and has the potential to be an effective tool for the stabilization of initial intermediates in the ozonolysis of alkenes. Several groups have tried this approach with limited success.[17] These studies have demonstrated that the careful control of the time and energy available for reaction is crucial. The present study uses three different deposition techniques to vary the reaction time and energy dissipation rates for the reaction of ozone with 2,3-dimethyl-2-butene (DMB).

Energy dissipation may come either through bimolecular collisions (such as with excess Ar) or by internal V → R → T energy transfer. The substituents on the alkene provide a means to control the number of internal degrees of freedom for the alkene involved in the reaction with ozone and thus the V → R → T energy transfer rate. DMB is a tetra-substituted alkene with a relatively high rate constant for a reaction with ozone (6.99×10^8 cm^3 mol^{-1} s^{-1}) at 298 K when compared to less substituted alkenes in general.[18] On the other hand, tetra-substituted alkenes in ozonolysis reactions are thought to form a CI with two methyl group substituents, making the recombination reaction to the SOZ more difficult.[19] As described below, the current study has led to the observation of the POZs and SOZs as well as the CI for the DMB/O$_3$ system.

Experimental Section

All of the experiments in this study were carried out on a conventional matrix isolation apparatus that has been described.[20] DMB (Acros, 98%) was introduced into the vacuum system as the vapor above the room temperature liquid, after
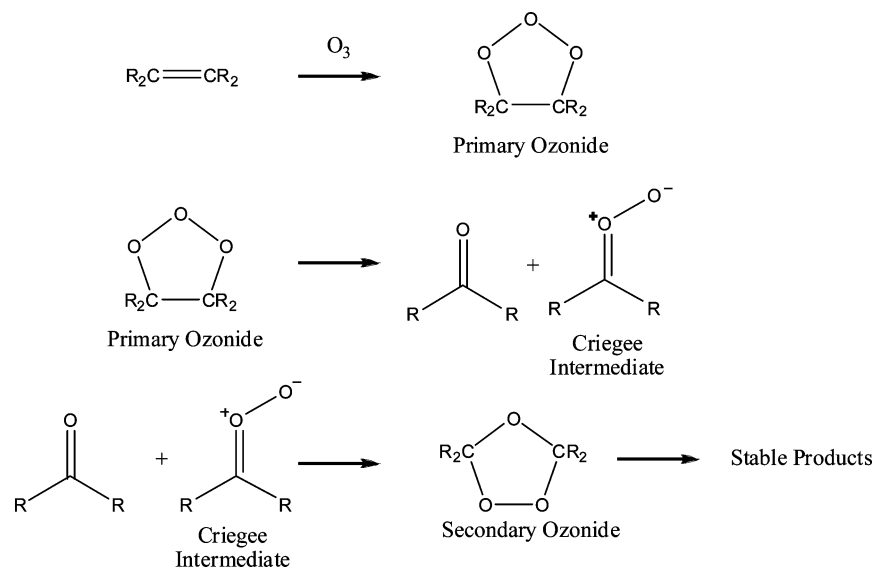

Figure 1. Criegee mechanism for the ozonolysis of alkenes.

purification by freeze−pump−thaw cycles at 77 K. $^{16}O_3$ was produced by Tesla coil discharge of $^{16}O_2$ (Wright Brothers) and trapping at 77 K to remove residual $^{16}O_2$ and trace gases. $^{18}O_3$ was produced in the same manner from oxygen-^{18}O (Cambridge Isotope Laboratories, 94%,). Scrambled $^{16,18}O_3$ was generated by discharging 50% $^{18}O_2$ with 50% $^{16}O_2$. In blank experiments, hydroxyacetone (Aldrich 90%) and acetone (Aldrich, 99%) were introduced into the vacuum system as the vapor above the room temperature liquid, after purification by freeze−pump−thaw cycles at 77 K. Argon (Wright Brothers) and in some cases O_2 (Wright Brothers) were used as the matrix gases without further purification.

Matrix samples were deposited in the twin, merged, and concentric jet modes. In the first, the two gas samples were deposited from separate nozzles onto the 19 K window, allowing for only a very brief mixing time prior to matrix deposition. Several of these matrixes were subsequently warmed or annealed to 35 K to permit limited diffusion and/or reaction. These matrixes were then recooled to 19 K and additional spectra recorded. In addition, the twin jet matrixes were irradiated for 1.0 h with the H_2O/quartz-filtered output of a 200 W medium-pressure Hg arc lamp, after which further spectra were recorded. Using a variety of coated quartz filters, a number of the twin jet experiments were irradiated with wavelengths ranging from $\lambda \geq 220$ to ≥ 580 nm.

Many experiments were conducted in the merged jet mode, in which the two deposition lines were joined with an UltraTorr tee at a predetermined distance from the cryogenic surface, and the flowing gas samples were permitted to mix and react during passage through the merged region. The length of this region was approximately 2.0 m for this study.

Twin and merged jet depositions probe different time scales for reaction, very short for twin jet and somewhat longer for merged jet. To probe the intermediate time scale between twin and merged jets, a new concentric jet device was developed. In this approach, an 1/8 in. o.d. Teflon FEP tube was inserted inside of a larger 1/4 in. o.d. tube, also Teflon FEP. The length of the 1/8 in. tube could be adjusted to be shorter, longer, or the same as the outer tube. The distance between the outlet ends of the two tubes is referred to as $\Delta d =$ (position of inner tube) − (position of outer tube); $d > 0$ indicates that the inner tube extends beyond the outer tube (more like twin jet), and $d < 0$ indicates that the inner tube is shorter than the outer tube (more

like merged jet). The $d = 0$ indicates that the ends of the two tubes are at the same distance from the cold window. Mixing of the two samples begins at the outlet of the inner tube and continues until deposition onto the cold window (typically 2−3 cm). In this manner, the time scale available for reaction could be adjusted from nearly that of the merged jet to nearly that of the twin jet. In all three modes, matrixes were deposited at the rate of 2 mmol/h from each sample manifold onto the cold window. Final spectra were recorded on a Perkin−Elmer Spectrum One Fourier transform infrared (IR) spectrometer at 1 cm^{-1} resolution.

Theoretical calculations were carried out on the possible intermediates, final and photochemical products in this study, using the Gaussian 03 and 03W suite of programs.[21] Density functional calculations using the hybrid B3LYP functional were used to locate energy minima, determine structures, and calculate vibrational spectra. Final calculations with full geometry optimization employed the 6-311G ++(d,2p) basis set, after initial calculations with smaller basis sets were run to approximately locate energy minima.

Results

Prior to any deposition experiments, blank experiments were run on each of the parent reagents used in this study. Hydroxyacetone and acetone blank spectra were also obtained for comparison with experimental spectra (Figures S1 and S2, Supporting Information). In each case, the blanks were in good agreement with literature spectra.[22,23]

Twin Jet $^{16}O_3$ + DMB. A series of twin jet experiments were conducted with samples of Ar/O_3 = 250 and Ar/DMB = 250. In a typical experiment, a number of new bands were observed after 19.0 h of deposition. The matrix was then annealed to 35 K and recooled to 19 K. A spectrum was then recorded, and the new absorptions grew by approximately 200%; these are listed in Table 1 and seen in Figure 2. The experiment was repeated several times, using different sample concentrations varying from M/R (matrix/reactant) = 167 to M/R = 500. The results were reproducible, with product band intensities that varied proportionally with sample concentrations. Then, the annealed matrix was irradiated for 1.0 h with the filtered ($\lambda \geq$ 220 nm) output of a medium-pressure Hg arc lamp. This produced many new product bands, shown in Figure 3; Table

TABLE 1: Band Positions and Assignments for the Initial Intermediates in the Thermal Reaction of O_3 with DMB

exptl. bands[a]	calcd. bands[b]	calcd. shift	exptl. shift	assignment
		^{18}O		
650	647	−7	−8	POZ
691	689	−27	−27	POZ
729	760	−40	−39	POZ
829	827	−31	−32	SOZ
842	841	−24	−22	POZ
854	865	−25	−11	POZ
870	848	−20	−33	SOZ
880	854	−44	−34	CI
949	952	−4	0	POZ
1092	1017	0/−7	0/−7	POZ/acetone
1141				POZ[c]
1146	1160	−2	−3	POZ
1154	1177	−2	−2	POZ
1195	1184	−1	0	POZ
1206	1223	−4	−4	SOZ
1245	1224	−1	0	POZ
1349	1388	0	0	acetone
1354	1465	0	0	acetone
1362	1469	0	0	acetone
1370	1475	−2	0	acetone
1393	1403	−1	0	POZ
1422				acetone[c]
1489	1491	0	−3	POZ
1713				acetone[c]
1718	1785	−35	−33	acetone

[a] Frequencies in cm^{-1}. [b] Calculated at the B3LYP/6-311G++(d,2p) level of theory. [c] Assignments based on literature for POZ and blank spectra for acetone.

2 shows the full list of product absorptions produced as a result of irradiation. Several product bands that were present before irradiation decreased after irradiation. In one experiment, the wavelength of irradiation was varied from $\lambda \geq 580$ to ≥ 220 nm. Product bands present before irradiation decreased, and new bands that grew in became more intense when irradiating from longer to shorter wavelengths. In the cases where O_2 was used as a matrix material, the absorptions that resulted from irradiation were much more intense than those when Ar was used (Figure S3, Supporting Information).

Merged Jet $^{16}O_3$ + DMB. Initial merged jet experiments were conducted with samples of $Ar/O_3 = 250$ and $Ar/DMB =$ 250 using a 2.0 m merged or reaction region held at room temperature. This configuration allows for an increased gas-phase reaction time for the reactions relative to twin jet deposition and prior to matrix deposition. In each of the merged jet experiments, the parent bands of both reagents were substantially reduced in intensity, indicating that a reaction was occurring. In addition, many new product bands were observed throughout the spectrum, including several intense bands in the carbonyl stretching region. Figure S4 (Supporting Information) shows a portion of the spectrum from one merged jet experiment. Some of the new bands were similar to those in the twin jet experiments, but the bands were generally more similar to the twin jet irradiation experiments. These bands were reproduced in several experiments, all with the merged region held at room temperature. Additional merged jet experiments were conducted, varying both reactants from M/R (matrix/reactant) = 167 to M/R = 500. These experiments provided a variation in product concentration without compromising dilution ratios and subsequent secondary reactions. Product absorption intensities were directly proportional to this variation of reactant concentrations.

Concentric Jet $^{16}O_3$ + DMB. The reaction of ozone with DMB was explored in several concentric jet experiments as well, all with concentrations of 250:1 for each reagent and *d* ranging from −11.0 to +1.0 cm. Table S1 (Supporting Information) lists the intensities of three important bands from the twin jet experiment. The intensities of the bands at 729, 1206, and 1721 cm^{-1} were monitored as a function of *d* in the concentric jet experiments. In an experiment with *d* = +1 cm, many of the bands from the twin jet annealed experiment were seen, although with much less intensity. When an experiment was conducted with *d* = 0 cm, similar results were seen with even lower intensities. Going from *d* = 0 to −1 cm, the three bands monitored increased slightly at similar rates. From *d* = −1 to −6 cm, both bands at 729 and 1721 cm^{-1} decreased, while the 1206 cm^{-1} band increased. Figure S5 (Supporting Information) shows representative regions at *d* = −1 and −6 cm. From *d* = −6 to −11 cm, a dramatic decrease in the three bands was observed. No new bands (i.e., bands not seen in either twin or merged jet experiments) were seen in these experiments.

$^{18}O_3$ + DMB. Twin, merged, and concentric jet experiments were also conducted with samples of $Ar/^{18}O_3 = 250$ deposited with samples of $Ar/DMB = 250$. Results paralleled those
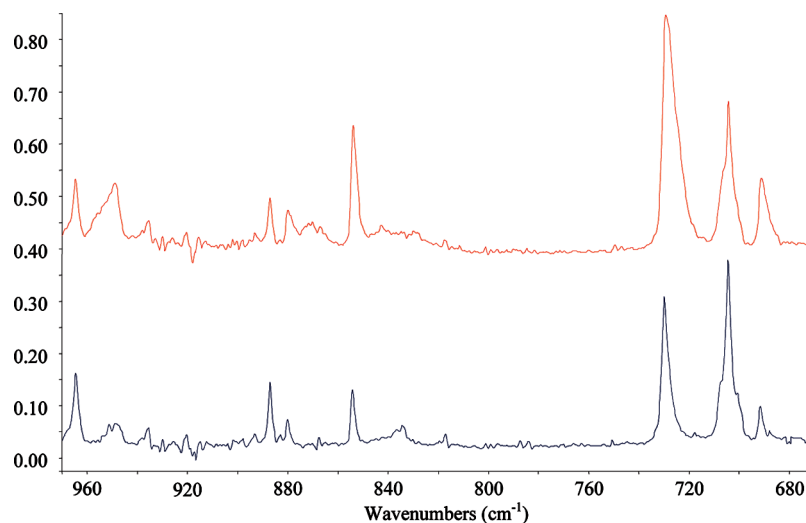

Figure 2. Select region of IR spectra from twin jet deposited $Ar/^{16}O_3/DMB = 500:1:1$. The blue trace is after 19 h of depositing. The red trace is after annealing to 35 K.
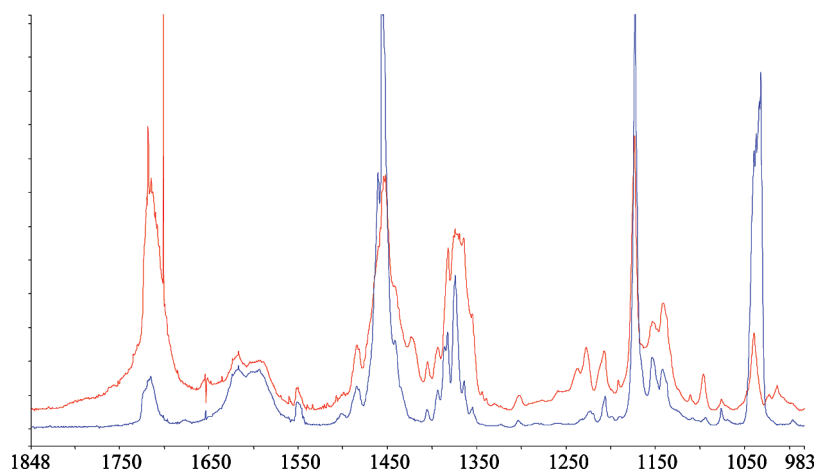
Figure 3. IR spectra of twin jet deposited $O_2/O_3/DMB = 500:1:1$. The blue trace is after depositing for 19 h. The red trace is the result from irradiating with $\lambda \geq 220$ nm.

TABLE 2: Band Positions and Assignments for New Product Absorptions from the Twin Jet Deposition of Ozone with DMB upon Irradiation with Light of $\lambda \geq 220$ nm

exptl.[a]	literature (Ar matrix)[b]	assignment
655	656	HA
846	847/848	TMO/MA
900	899[c]	DMDO
1022	1094[c]	DMDO
1093	1095/1092	HA/AC
1142	1142	TMO
1206	1205	TMO
1224	1217	AC
1244	1245	FOR
1256	1228	HA
1283	1286	HA
1301	1302	CH₄
1330	1209[c]	DMDO
1354	1354/1354	PC/AC
1363	1362	AC
1373	1369/1361/1370	PC/HA/MA
1380	1381	TMO
1404	1406/1407	TMO/AC
1422	1422/1407	PC/AC
1440	1438/1439/1444	TMO/PC/AC
1450	1452	AC
1460	1462	MA
1489	1471	TMO
1712	1713	PC
1718	1722/1717	AC/PC
1733	1731	HA
1756	1761	MA
2136	2138/2138	CO/FOR
3431br	3505	HA

[a] Frequencies in cm^{-1}. *[b]* References 22, 23, 25, 29, 31, 34, and 35. *[c]* Liquid-phase IR spectra. HA = hydroxyacetone, TMO = tetramethyloxirane, PC = 3,3-dimethyl-2-butanone, AC = acetone, MA = methyl acetate, CO = carbon monoxide, FOR = formaldehyde, and DMDO = dimethyldioxirane.

obtained for the normal isotopic species, with many product bands showing an isotopic shift relative to the corresponding $^{16}O_3$ experiments. Many product bands were observed, some of which were slightly less intense than the pure ^{16}O corresponding bands, while the parent bands were reduced.

Multiple twin jet experiments were conducted with samples of Ar/DMB = 250 codeposited with Ar/$^{16,18}O_3$ = 250. The resulting product bands were less intense than those in the pure $^{16}O_3$ and $^{18}O_3$ experiments, while several new, less intense bands were present. The positions and assignments for these bands are given in Table 3.

Results of Calculations

To complement the experimental data, DFT calculations were carried out on all intermediates and possible products. An energy minimum was located for the optimized structures, and the vibrational spectra were calculated for both normal isotope species in oxygen containing molecules and ^{18}O-substituted isotopomers. Calculated structures for the anticipated intermediates of interest and additional possible products are presented in Figures 4 and S6 (Supporting Information).

Key structural parameters for the CI in comparison with the similar acetone molecule can been seen in Table S2 (Supporting Information). Of particular importance are the calculated vibrational frequencies and intensities for the POZ, CI, and SOZ; these are listed in Table 1. In addition to the fundamental absorptions for each species, the ^{18}O shifts of the most intense absorptions for each species are very valuable when comparing to experimental data. For the POZ, the most intense absorption is calculated at 760 cm^{-1} with a -40 cm^{-1} ^{18}O shift. This is ascribed to the O−O−O antisymmetric stretching mode. The characteristic O−O stretch of the CI was calculated at 910 cm^{-1} with a -44 cm^{-1} shift with ^{18}O. The most intense absorption of the SOZ was calculated at 1223 cm^{-1} with a smaller ^{18}O shift of -4 cm^{-1} and is associated with a C−O−C stretching motion. These theoretical calculations were compared to the experimental observations from twin, merged, and concentric jet deposition experiments.

Discussion

An important goal in the current study of the ozone/DMB system is to provide experimental evidence for the reaction mechanism by the direct observation of the early intermediates. In particular, Criegee predicted the formation of a POZ, (which has been observed previously),[24] as well as the CI and the SOZ. These latter two species have not been observed experimentally in studies of the ozonolysis of DMB.[19] The POZ may decompose rapidly, forming acetone, a species whose infrared spectrum in an argon matrix has been reported,[23] and the CI. Because the starting alkene is symmetrical, the acetone/CI pair may recombine to form a single SOZ or may separate and undergo stabilizing collisions.

O₃ + DMB Twin Jet. Twin jet, merged jet, and concentric jet deposition were used to probe different time and temperature regimes with respect to the mixing and reacting of O₃ with DMB. Twin jet deposition allows for only a brief amount of

TABLE 3: Product Band Positions and Assignments for the Intermediates in the Ozonolysis of DMB

experimental position[a] and shifts						calculated[b] position and shifts									
^{16}O	$\Delta^{16,18}O$				$\Delta^{18}O$	^{16}O	$\Delta^{16,18}O$						$\Delta^{18}O$	assignment
729	−11	−15	−22	−26	−39	760	−12	−17	−23	−28			−40	POZ
854	−3	−5			−11	865	−1	−5	−16	−24			−25	POZ
870					−33	848	−4	−4	−6	−6	−17	−17	−20	SOZ
880	−12	−20			−34	910	−18	−25					−44	CI
1206					−4	1223	−1	−1	−2	−3	−3	−3	−4	SOZ
1718					−33	1785							−35	acetone

[a] Band positions in cm^{-1}. [b] Calculated using the B3LYP 6-311G ++ (d,2p) level of theory.
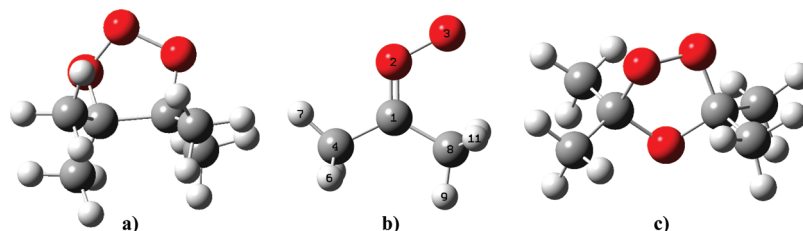

Figure 4. Calculated structures for the (a) POZ, (b) CI, and (c) SOZ from the reaction of ozone with DMB.

mixing on the surface of the condensing matrix surface. Upon initial twin jet deposition, a number of moderately weak absorptions were observed, as listed in Table 1. Annealing these matrixes to 35 K resulted in the substantial growth (~200% increase) of these absorptions. These observations indicate that reaction is occurring at 35 K and that the barrier to this reaction must be very low ($3/2RT \approx 0.1$ kcal mol^{-1} at 35 K). Also, the formation of approximately 30 product bands strongly suggests that more than one species is being formed. In addition, the bands in these twin jet experiments were different than those observed in the merged jet experiment, where most of the products were the anticipated to be stable oxidation products. Likewise, the product bands observed in the these twin jet experiment were entirely different than those in the irradiation experiments, where photochemical products were observed. These results are in agreement with recent studies from this laboratory on related systems.

As outlined below, substantial evidence supports the assignment of product absorptions in Table 1 to the POZs and SOZs of DMB, as well as to the CI−acetone pair. First, direct comparison between several of these experimental absorptions to the POZ absorptions reported in the literature supports formation of the POZ. For example, the most intense literature bands for the POZ are at 729 and 1146 cm^{-1}.[24] Relatively intense bands were observed in the current study at those same positions, as seen in Table 1. In addition, while the previous study did not incorporate ^{18}O labeling or theoretical calculations, these were an integral part of the present study. Theoretical calculations for the ^{18}O-labeled POZ predict a −40 cm^{-1} isotopic shift for the intense absorption at 760 cm^{-1} (calculated, unscaled). The experimental band at 729 cm^{-1} was in excellent agreement with this prediction, with a −39 cm^{-1} ^{18}O shift. Further, six bands were anticipated in the scrambled $^{16,18}O_3$ experiments, and all six were observed. These can be seen in Table 3. Finally, there was good agreement between experimental observations and theoretical calculations for all observed vibrational bands of the POZ and their corresponding ^{18}O shifts. *Thus, the POZ of DMB is clearly formed, isolated, and detected in these experiments.*

A second key conclusion comes from the comparison between these twin jet spectra and a blank infrared spectrum of acetone in argon (Figure S1, Supporting Information). This comparison strongly supports the formation of acetone upon initial deposition

and its growth upon annealing to 35 K. All of the most intense bands of acetone were observed in the twin jet experiments and showed the anticipated ^{18}O shifts. Of note, the C=O stretch at 1718 cm^{-1} was the most intense product absorption in the twin jet experiment and was slightly shifted (4−5 cm^{-1}) compared to the blank acetone experiment. This is thought to be from an interaction between the acetone molecule and CI in the argon cage. The ^{18}O shift of this band, −33 cm^{-1}, was the anticipated shift. In addition, both acetone isotopomers at 1718 and 1685 cm^{-1} were observed in the $^{16,18}O_3$ scrambled experiments, demonstrating the presence of a single O atom in this product species.

One additional product band in the twin jet experiments was a weak band that was consistently observed at 880 cm^{-1}. This band shifted −34 cm^{-1} to 846 cm^{-1} with ^{18}O labeling. In addition, when 50% scrambled $^{16,18}O_3$ was employed, a quartet of nearly equally intense bands was observed at 880, 868, 860, and 846 cm^{-1}, as can be seen in Figure S7 (Supporting Information). The most apparent origin of an isotopic quartet is from a species with two inequivalent oxygen atoms. The CI, a carbonyl oxide (see Figure 1), is one of a relatively few species that meets this requirement. Moreover, the antisymmetric C=O−O stretching mode (often described as an O−O stretch) has been observed for carbonyl oxides in the vicinity of 900 cm^{-1} and was observed at 922 cm^{-1} for the CI of *cis*-2-butene.[13]

Theoretical calculations predict that the most intense band of the CI will come at 910 cm^{-1} (unscaled) with a 44 cm^{-1} ^{18}O shift. This matches well the observed band and shift, taking into account that such calculations are typically 3% too high. Moreover, the positions of the two intermediate isotopic bands at 860 and 868 cm^{-1} are well-reproduced by calculations. It is noteworthy that calculations predict only a single intense band for the CI, along with a number of quite weak bands. Thus, the observation of a single product band is in keeping with the prediction of the calculations.

Other possible products that might form from the rearrangement and stabilization of the CI include hydroxyacetone via internal O atom transfer or methyl acetate through a dioxirane intermediate.[19] However, these are species for whom infrared spectra are available[22,25] (a blank was run on hydroxyacetone in solid argon to provide an authentic sample). The key infrared absorptions of these species were entirely absent. Moreover, they have no absorptions that could account for the product band

at 880 cm⁻¹. Finally, these unimolecular stabilization pathways have activation energies calculated to range from approximately 10 to 20 kcal mol⁻¹.[26] Thus, these pathways are much less likely and do not appear to play a role under the present experimental conditions.

Finally, the Criegee mechanism predicts the formation of the CI along with acetone from the decomposition of the POZ of DMB. In view of the definitive observation of acetone (see above), the very good agreement of calculation and experiments for the C=O−O stretch mode and, overall, the observation of an isotopic quartet in the scrambled ¹⁶,¹⁸O₃ experiments, and the lack of observation of anticipated rearrangement products of the CI, *the evidence collectively supports assignment of the 880 cm⁻¹ band to the CI of DMB*. Further, this provides definitive evidence that tetra-substituted alkenes follow the Criegee mechanism.

Earlier studies have suggested that formation of a SOZ from the CI of tetra-alkyl-substituted alkenes would be more difficult than that from a lesser substituted alkene.[19] Later studies have disputed this suggestion. While the SOZ of DMB has not been reported in the gas phase or in inert matrixes, one study reported the observation of this species immobilized in a polyethylene film.[27] However, this study lacked isotopic labeling and theoretical calculations, and the broad spectral features made this identification tentative. In the present study, additional weak product absorptions were observed at 1206, 870, and 829 cm⁻¹. Incorporation of ¹⁸O labeling and comparison to theoretical calculations for the SOZ provide good evidence that these bands can be assigned to the SOZ of DMB. In particular, the most intense calculated absorption for the SOZ came at 1223 cm⁻¹ with a −4 cm⁻¹ calculated ¹⁸O shift without scaling. This corresponds nicely to the most intense experimental absorption for the SOZ at 1206 cm⁻¹ that had an ¹⁸O shift of −4 cm⁻¹. Similar agreement of experiment and theory was seen for the 829 and 870 cm⁻¹ bands, as shown in Table 1. While many more bands are anticipated for the SOZ, additional absorptions were not observed in part due to overlap with parent bands in the reaction spectrum and in part due to low intensities. No additional bands were observed for the SOZ in the ¹⁶,¹⁸O₃ mixed isotope experiment. Considering that there are eight calculated isotopomers for each SOZ band, the intensities of each individual band in the experimental study would be greatly reduced to the point that they would not be observed. Table 3 shows calculated positions for the SOZ isotopomers.

O₃ + DMB Twin Jet Photochemistry. In twin jet argon matrix experiments that were irradiated with light of λ ≥ 220 nm, the absorptions listed above for the early intermediates decreased, and several new weak product bands were observed. When the same experiment was conducted with O₂ as the matrix material, the same new photochemical product absorptions were observed and with increased intensity (Figure S3, Supporting Information). These results indicated that two different processes were occurring. First was the decomposition of the early intermediates, and second was the photodetachment of an O atom from ozone upon irradiation followed by O atom reaction with an available substrate molecule. The reaction of O atoms with alkenes has been proposed to occur as shown in Figure 5, with O atom attack occurring at the less substituted carbon atom in the double bond.[28] This can lead to either stabilization and formation of the appropriate ketone (3,3-dimethyl-2-butanone in the system under study here) or the formation of a three-membered epoxide ring.

Using O₂ as the matrix material is thought to increase mobility of the O atoms and, as a result, increase the likelihood
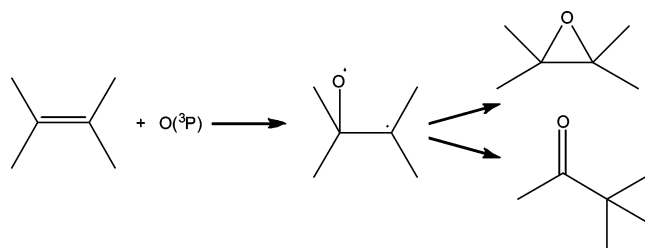

Figure 5. Scheme for the O atom attack on the double bond of DMB.

that the O atom will find a substrate molecule and react. Most of the observed product absorptions that grew in when irradiated from λ ≥ 220 to ≥580 nm can be assigned to either acetone, tetramethyloxirane, or 3,3-dimethyl-2-butanone based on literature spectra and theoretical calculations.[23,29]

It is noteworthy that the 880 cm⁻¹ band assigned to the CI was reduced in intensity when irradiated with light with λ < 550 nm. At the same time, several new absorptions were observed when irradiating in this wavelength range. These included two weak carbonyl stretch absorptions at 1733 and 1756 cm⁻¹ and a broad O−H stretch at 3431 cm⁻¹. These observations suggest destruction of the CI and formation of related products. As discussed above, unimolecular rearrangement products, including hydroxyacetone, dioxirane, and methyl acetate, are likely candidates. In this case, the energy required for the CI to overcome the calculated 10−20 kcal mol⁻¹ barrier leading to these stable compounds is available through absorption of light. Sander found that while generating carbonyl oxides (CIs) via another route, irradiation at select wavelengths led to different products (λ = 515 nm leads to dioxirane formation and further to an ester at λ = 438 nm).[30] In similar manner, the bands observed here at 1733, 1756, and 3431 cm⁻¹ are assigned to hydroxyacetone and methyl acetate. In addition, there are three weak bands at 900, 1022, and 1330 cm⁻¹ assigned to the dioxirane[31] that serves as an intermediate between the CI and methyl acetate. In Figure 6, the CI band at 880 cm⁻¹ decreases as the dioxirane band at 900 cm⁻¹ increases. *These results present direct evidence of the wavelength dependence of the photodestruction of a CI.*

O₃ + DMB Merged Jet. In merged jet deposition, the mixing of ozone and DMB occurred at room temperature in a flow tube outside of the matrix cell. Additional reaction time is available in this mode compared to that in twin jet and has led to "late" thermal reaction products in previous studies. In these experiments, bands of the precursors and early intermediate species decreased significantly compared to those in twin jet spectra, and a number of new product absorptions were observed. This indicates that extensive reaction occurred during the transit through the merged jet or reaction region. In particular, there were numerous product bands in the carbonyl stretching region as well as a broad absorption at 3497 cm⁻¹, suggesting the presence of an O−H-containing species. Product identification can be made from the known infrared spectra in Ar matrixes for methyl glyoxal, hydroxyacetone, acetone, tetramethyloxirane, and 3,3-dimethyl-2-butanone.[22,23,29,32] While mostly stable products were formed, these are consistent with the Criegee mechanism and secondary reactions of the CI. The observation of tetramethyloxirane and 3,3-dimethyl-2-butanone in this system may be the result of the loss of an O atom from the CI and subsequent reaction with the alkene. Other final products are in agreement with a related gas-phase study of the reaction of DMB with ozone at room temperature in a static system with rapid mixing that yielded methyl glyoxal, methyl acetate, and hydroxyacetone as major products. Niki et al. noted that the
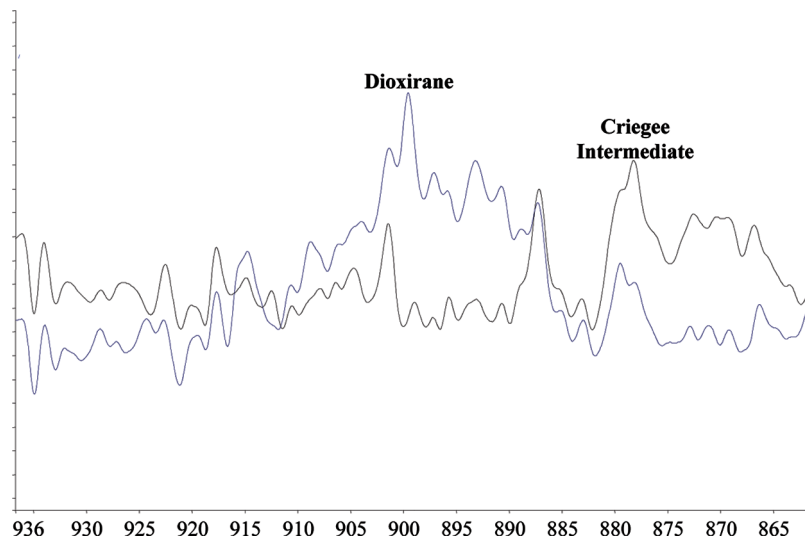
Figure 6. IR spectra of twin deposited Ar/$^{16}O_3$/DMB = 500:1:1. The black trace is the spectrum upon annealing to 35 K. The blue trace is upon irradiation with $\lambda \geq 220$ nm.

presence of these carbonyl compounds in normal gas-phase conditions is a result of further reactions of the CI and not decomposition of the SOZ.[33] Not only do these results give additional evidence for the Criegee mechanism, but more importantly, they show the formation and rearrangement of the CI.

O$_3$ + DMB Concentric Jet. In concentric jet experiments, the relative amounts of the intermediates can be monitored by the intensity of infrared absorptions assigned to each species as a function of system geometry. All of the absorptions for the POZ, SOZ, and acetone seen in twin jet experiments were observed using concentric jet; the more intense absorptions for each species were monitored. While the 880 cm^{-1} band of the CI was too weak to monitor in these concentric jet experiments, the behavior of the acetone band will serve to probe the behavior of the CI/acetone pair. As discussed above, bands at 729, 1721, and 1206 cm^{-1} have been assigned to the POZ, acetone, and SOZ, respectively, and were used to monitor the relative amounts of these three intermediates. In concentric jet experiments with $d \geq 0$, the results were very similar to those of the twin jet, with the observation of these three bands but with slightly less intensity. As d became negative from -1 to -6 cm, the bands associated with the POZ and acetone decreased, and the SOZ yield increased. From $d = -6$ to -11 cm, the three bands decreased as the merged jet products (carbonyl compounds) increased dramatically, suggesting that this geometry approached that of merged jet deposition. No entirely new bands were observed using any value of d; therefore, the concentric jet was able to successfully transition between the twin and merged jet regimes. Following the mechanism in Figure 1, as the SOZ is formed, there should be a decrease in the POZ, CI (although not seen here), and acetone. The observations here are consistent with this mechanism.

Conclusions

The codeposition of O$_3$ with DMB into Ar matrixes under varying conditions has led to the observation of the early reaction intermediates and stable reaction products. Twin jet deposition followed by warming to 35 K led to moderately intense product bands assigned to the POZ, SOZ, CI, and acetone. The DMB POZ has been observed and characterized previously; the present study enhanced the earlier work with the addition of ^{18}O isotopic labeling and theoretical calculations. *The formation and isolation of the CI resulting from a tetra-substituted alkene increases the overall understanding of the mechanism of the ozonolysis of alkenes.* The identification and spectroscopic characterization of the SOZ of DMB in argon matrixes was successful as well. Irradiation of these matrixes resulted in products formed from the unimolecular rearrangement of the CI, photodestruction of the POZ and SOZ, and O atom attack on DMB. The formation of both hydroxyacetone and methyl acetate in the photochemical studies suggests a rearrangement of the CI. In contrast, merged jet deposition led a variety of carbonyl-containing final products, depending on the length of the flow reactor.

Supporting Information Available: Additional experimental spectra, calculated spectra, calculated molecular structures, and data tables. This material is available free of charge via the Internet at http://pubs.acs.org.

References and Notes

(1) Ravishankara, A. R. *Chem. Rev.* **2003**, *103*, 4505.
(2) Slanger, T. C.; Copeland, R. A. *Chem. Rev.* **2003**, *103*, 4731.
(3) Olzmann, M.; Kraka, E.; Cremer, D.; Gutbrod, R.; Andersson, S. *J. Phys. Chem. A* **1997**, *101*, 9421–9429.
(4) Horie, O.; Moortgat, G. K. *Atmos. Environ., Part A* **1991**, *25A*, 19881–1896.
(5) Grosjean, E.; Grosjean, D. *Environ. Sci. Technol.* **1996**, *30*, 1321.
(6) Atkinson, R.; Tuazon, E. C.; Aschmann, S. M. *Environ. Sci. Technol.* **1995**, *29*, 1860.
(7) Criegee, R. *Rec. Chem. Prog.* **1957**, *18*, 111.
(8) Criegee, R. *Angew. Chem.* **1975**, *87*, 765.
(9) Chan, W.-T.; Hamilton, I. P. *J. Chem. Phys.* **2003**, *118*, 1688–1701.
(10) Hendricks, M. F. A.; Vinckier, C. *J. Chem. Phys. A* **2003**, *107*, 7574–7580.
(11) Ljubic, I.; Sabljic, A. *J. Phys. Chem. A* **2002**, *106*, 4745–4757.
(12) Anglada, J. M.; Crehuet, R.; Bofill, J. M. *Chem.—Eur. J.* **1999**, *5*, 1809–1822.
(13) Clay, M.; Ault, B. S. *J. Phys. Chem. A* **2010**, *114*, 2799–2805.
(14) Hoops, M. D.; Ault, B. S. *J. Am. Chem. Soc.* **2009**, *929*, 22.
(15) Cradock, S.; Hinchcliffe, A. J. *Matrix Isolation*; Cambridge University Press: Cambridge, U.K., 1975.

12674 *J. Phys. Chem. A, Vol. 114, No. 48, 2010*

Coleman and Ault

(16) Andrews, L.; Moskovits, M.; Eds. *Chemistry and Physics of Matrix-Isolated Species*; Elsevier Science Publishers: Amsterdam, The Netherlands, 1989.

(17) (a) Kohlmuller, C. K.; Andrews, L. *J. Am. Chem. Soc.* **1981**, *103*, 2578–2583. (b) Hawkins, M.; Kohlmuller, C. K.; Andrews, L. *J. Phys. Chem.* **1982**, *86*, 3154–3166. (c) Andrews, L.; Kohlmuller, C. K. *J. Phys. Chem.* **1982**, *86*, 4548–4557. (d) Clark, R. J. H.; Foley, L. J. *J. Phys. Chem. A* **2002**, *106*, 3356–3364. (e) Feltham, E. J.; Almond, M. J.; Marston, G.; Ly, V. P.; Wiltshire, K. S. *Spectrochim. Acta, Part A* **2000**, *56A*, 2605–2616.

(18) Atkinson, R.; Carter, W. *Chem. Rev.* **1984**, *84*, 437–470.

(19) Bailey, P. *Ozonation in Organic Chemistry Olefinic Compounds*; Academic Press, Inc.: New York, 1978.

(20) Ault, B. S. *J. Am. Chem. Soc.* **1978**, *100*, 2426.

(21) Frisch, M. J.; Trucks, G. W.; Schlegel, H. B.; Scuseria, G. E.; Robb, M. A.; Cheeseman, J. R.; Montgomery, J. A., Jr.; Vreven, T.; Kudin, K. N.; Burant, J. C.; Millam, J. M.; Iyengar, S. S.; Tomasi, J.; Barone, V.; Mennucci, B.; Cossi, M.; Scalmani, G.; Rega, N.; Petersson, G. A.; Nakatsuji, H.; Hada, M.; Ehara, M.; Toyota, K.; Fukuda, R.; Hasegawa, J.; Ishida, M.; Nakajima, T.; Honda, Y.; Kitao, O.; Nakai, H.; Klene, M.; Li, X.; Knox, J. E.; Hratchian, H. P.; Cross, J. B.; Bakken, V.; Adamo, C.; Jaramillo, J.; Gomperts, R.; Stratmann, R. E.; Yazyev, O.; Austin, A. J.; Cammi, R.; Pomelli, C.; Ochterski, J. W.; Ayala, P. Y.; Morokuma, K.; Voth, G. A.; Salvador, P.; Dannenberg, J. J.; Zakrzewski, V. G.; Dapprich, S.; Daniels, A. D.; Strain, M. C.; Farkas, O.; Malick, D. K.; Rabuck, A. D.; Raghavachari, K.; Foresman, J. B.; Ortiz, J. V.; Cui, Q.; Baboul, A. G.; Clifford, S.; Cioslowski, J.; Stefanov, B. B.; Liu, G.; Liashenko, A.; Piskorz, P.; Komaromi, I.; Martin, R. L.; Fox, D. J.; Keith, T.; Al-Laham, M. A.; Peng, C. Y.; Nanayakkara, A.; Challacombe, M.; Gill, P. M. W.; Johnson, B.; Chen, W.; Wong, M. W.; Gonzalez, C.; Pople, J. A. *Gaussian 03*, revision B.04; Gaussian, Inc.: Pittsburgh, PA, 2003.

(22) Sharma, A.; Reva, I.; Fausto, R. *J. Phys. Chem. A* **2008**, *112*, 5935–5946.

(23) Cosani, K. *J. Phys. Chem.* **1987**, *91*, 5586–5588.

(24) Samuni, U.; Haas, Y.; Fajgar, R.; Pola, J. *J. Mol. Struct.* **1998**, *449*, 177–201.

(25) Patten, K.; Andrews, L. *J. Phys. Chem.* **1986**, *90*, 1073–1076.

(26) Epstein, S.; Donahue, N. *J. Phys. Chem. A* **2008**, *112*, 13535–13541.

(27) Griesbaum, K.; Volpp, W.; Greinert, R.; Greunig, H.; Schmid, J.; Henke, H. *J. Org. Chem.* **1989**, *54*, 383–389.

(28) Cvetanovic, R. *Can. J. Chem.* **1958**, *36*, 623.

(29) Nakata, M. *Spectrochim. Acta, Part A* **1994**, *50A*, 1455–1465.

(30) Wierlacher, S.; Sander, W.; Marquardt, C.; Kraka, E.; Cremer, D. *Chem. Phys. Lett.* **1994**, *222*, 319.

(31) Murray, R. *Chem. Rev.* **1989**, *89*, 1187–1201.

(32) Mucha, M.; Saldyka, M.; Mielke, Z. *Pol. J. Chem.* **2009**, *83*, 943–956.

(33) Niki, H.; Savage, C.; Breitenbach, L.; Hurley, M. *J. Phys. Chem.* **1987**, *91*, 941–946.

(34) Diem, M.; Lee, E. *J. Phys. Chem.* **1982**, *86*, 4507–4512.

(35) Frayer, F.; Ewing, G. *J. Chem. Phys.* **1968**, *48*, 781.

JP108457W